# Circulating current control for parallel interleaved VSCs connected in whiffletree configuration

**L. Bede, G. Gohil, M. Ciobotaru, T. Kerekes, R. Teodorescu and V. G. Agelidis**


- ***Published in:*** IEEE 7th International Symposium on Power Electronics for Distributed Generation Systems (PEDG), Vancouver, BC, 2016
- ***DOI:*** 10.1109/PEDG.2016.7527091
- ***Publication date:*** 2016
- ***Citation for published version:*** L. Bede, G. Gohil, M. Ciobotaru, T. Kerekes, R. Teodorescu and V. G. Agelidis, "Circulating current control for parallel interleaved VSCs connected in whiffletree configuration," 2016 IEEE 7th International Symposium on Power Electronics for Distributed Generation Systems (PEDG), Vancouver, BC, 2016, pp. 1-6.

# Circulating Current Control for Parallel Interleaved VSCs Connected in Whiffletree Configuration

Lorand Bede[1], Ghanshyamsihn Gohil[1], Mihai Ciobotaru[2],Tamas Kerekes[1], Remus Teodorescu[1] ,Vassilios G Agelidis[2]
[1]Department of Energy Technology, Aalborg University Aalborg, Denmark
[2]School of Electrical Engineering and Telecommunications, University of New South Wales, Sydney, Australia
Email: lbe@et.aau.dk

*Abstract*— **This paper presents a Proportional Resonant (PR) based circulating current controller for four parallel interleaved Voltage Source Converters (VSCs). Interleaving the carrier signals will cause a switching frequency circulating current to flow between the VSCs. Therefore, to suppress these circulating currents the VSCs are interconnected through Coupled Inductors (CIs), which form a whiffletree configuration, and they are used to suppress the switching frequency circulating current. On the other hand, the CIs are highly sensitive to fundamental frequency circulating currents, which may saturate them. Hence, a circulating current controller is required, which effectively controls the fundamental component of the circulating current. Furthermore, the circulating current is sampled using a special technique, which does not require any additional. The effectiveness of the design methodology and the performance of the circulating current controller are verified by simulation and experimental results as well.**

***Keywords—Coupled Inductors, Interleaved VSC, Whiffletree, Circulating Current Control***

## I. INTRODUCTION

In 2015 in Denmark, 42% of the consumed electrical power was produced by wind turbine systems [1]. Such high penetration levels of distributed generation systems require more stringent standard requirements to keep the utility grid stable, such as the German BDEW standard [2]. The power generated by wind turbines is usually processed by Voltage Source Converters (VSCs) in order to meet the requirements of the demanding grid codes [3]. Furthermore, to reduce the cost of the plants, wind turbines with higher power ratings are installed [4, 5]. Generally, wind turbine systems use low voltage generators, meaning that in order to process the full power, several VSCs have to be connected in parallel to share the current between each other.

Total Harmonic Distortion (THD) of the resultant current can be reduced by interleaving the carrier signals of the parallel VSCs [6]. As a result, the filtering requirement for grid connected systems can be decreased, which in turn results in the reduction of size and weight [7, 8]. On the other hand, the carrier interleaving causes circulating currents to flow between the VSCs, which will increase both the conduction losses in the semiconductors, and copper losses in the inductive components [9]. The circulating current occurs when the upper switch of a phase of one VSC is connected to the positive DC link terminal and the lower switch of the corresponding phase in another VSC is connected to the negative DC link terminal, and vice-versa. During these instances the positive and negative terminals of the dc-link are short-circuited through the filter inductors.

Several methods exist on how to minimize the circulating current between VSCs. The circulating current can be completely eliminated between VSCs if an isolation transformer is used at the output of each VSC. On the other hand, this solution is not preferred due to the bulky line frequency transformer. The authors in [10] use Common Mode (CM) inductors, which are placed at the output of every VSC. [11]. However, this solution is not very effective in suppressing the circulating current. Another solution for this is to use Coupled Inductors (CIs). These CIs are placed between the corresponding phases of the VSCs and they only act on the high frequencies [12, 13]. The CI is designed to offer high inductance in the path of the high frequency circulating current, hence its size can be compact [14]. Usually the CI based solution is normally preferred, since it can outperform the other solutions in size and performance [14].

In this paper, four parallel interleaved VSCs are considered. In order to achieve symmetrical magnetic structure, the CIs are connected in a whiffletree configuration [15, 16], as shown in Fig. 1. The CIs in Converter Group 1 ($CG_1$) and $CG_2$ experience switching frequency excitations, while the CI in $CG_{12}$ experiences twice the switching frequency excitation. Assuming ideal current sharing between the VSCs, the fundamental frequency component of the flux is zero in the CI. As a result, CI can be designed for the high frequency flux excitation, therefore smaller size of the CI can be achieved [17, 18]. In practice however, equal current sharing is difficult to achieve because of unequal impedances between the parallel paths, dead-time[19], mismatches in the manufacturing, contact resistances, different turn on and turn off times of the VSCs etc. The unequal current sharing causes the flow of the low frequency circulating current. This low frequency circulating current has to be compensated, and failing to do so might saturate the CI, which will cause the VSCs to trip, and this should be avoided.

A method to eliminate the low frequency circulating current between two parallel interleaved VSCs is proposed in [20]. The use of a Proportional Resonant (PR) controller is proposed, in

978-1-4673-8617-3/16/$31.00 (c) 2016 IEEE

order to control the low frequency circulating current between the parallel VSC legs for each phase.

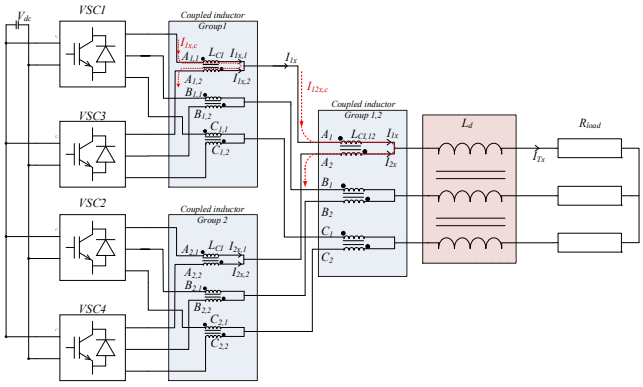


Fig. 1 Schematic of the system, with 4 converters in parallel with CIs connected in whiffletree configuration

Another solution is presented in [20], where multiple VSCs are interleaved. Here the authors ensure current sharing by calculating an average current for a corresponding phase, and based on this information the control signals are changed for each phase individually. However, this only controls the common mode current between the VSCs [21], and not the circulating current for each phase. Another solution is to use a dead beat circulating current controller as proposed in [22]. In this case the authors control the circulating current by modifying the common mode voltages applied to the VSCs

In this paper the authors present a method to control the fundamental frequency circulating current between the parallel VSCs, connected in a whiffletree configuration. The whiffletree configuration is shown in Fig. 1. Four VSCs are divided into two groups:

1) $CG_1$ comprises $VSC_1$ and $VSC_3$
2) $CG_2$ comprises $VSC_2$ and $VSC_4$

The carrier interleaving between the VSCs is set to be 90°. The CGs are comprised in a way that the interleaving angle between $VSC_1$ and $VSC_3$ is set to 180°, similarly the interleaving angle between $VSC_2$ and $VSC_4$ is also 180°. If the current sharing is not ideal between the VSCs within the same CG or between the CGs, fundamental frequency circulating current will flow through the CIs, which might saturate them, causing the VSCs to trip. In this article a PR based control method is proposed, in order to eliminate the fundamental frequency circulating current between the VSCs within each CG and between the CGs. Furthermore, a sampling method is also proposed, which ensures that the signal fed to the circulating current controllers only contains fundamental frequency components.

The article is structured as follows: after the Introduction, the System Description is given in Section II. In Section III, the Circulating Current Controller is presented. A sampling method, which does not require additional filtering to obtain the fundamental component of the circulating current is presented in Section IV while the Simulation and Experimental Results are shown in section V and section VI, respectively.

## II. System Description

### A. Converter system

The system under investigation consists of four parallel interleaved VSCs as presented on Fig. 1. The four VSCs can be separated into two groups, $CG_1$ ($VSC_1$ and $VSC_3$) and $CG_2$ ($VSC_2$ and $VSC_4$). The interleaving angle between the two VSCs in a CG is set to 180° and the VSC leg currents are sampled at the top and bottom update of the carrier signal. As a result the switching frequency component in the sampled circulating current can be naturally eliminated [18]. A CI is inserted between the parallel legs of the VSCs within each group, and it offers the inductance of $L_{CI}$ to the circulating current. Because of the interleaving angle of 180° between the CGs, additional circulating current will flow between the CGs. Hence, another CI ($L_{CI,12}$) is inserted between $CG_1$ and $CG_2$ for each phase, thus forming the whiffletree configuration.

### B. Circulating current

Switching frequency circulating current flows between the VSCs in a group, whereas the circulating current which flows between the CGs has a major frequency component at twice the switching frequency. Both of these circulating currents may contain fundamental frequency components as well, if mismatches exist. These mismatches between the VSCs and CGs can be caused by multiple sources[20], such as:

1) Difference in the control signals applied to the VSCs;
2) Mismatches between the turn on/off of the employed semiconductors;
3) Mismatches in the CI parameters due to manufacturing;
4) Differences in the cable parameters used to interconnect the VSCs
5) Mismatches in the current sensors

As presented in [20], all of these mismatches can be assumed as a series resistance.

Furthermore, the circulating currents can be expressed as follows:

$$I_{Yx,c} = \frac{I_{Yx,1} - I_{Yx,2}}{2} \tag{1}$$

where Y = [1,2,12] represents the number of the group, and *x* denotes the corresponding phase (x=[A,B,C]).

### C. Total Current Control

The total current ($I_{Tx}$) is controlled by using a PR controller in the $\alpha\beta$ reference frame. The benefit of this control algorithm is that it compensates for both positive and negative sequence currents and it has a high gain at the resonance frequency [21]. Furthermore, the asymmetrical regularly sampled approach is used, which means that the sampling and the control algorithm is run at the top and the bottom of the carrier signal, and that the sampled current will only have fundamental component values [22]. The carriers of the 4 VSCs are presented by Fig. 2, which shows that the top and bottom updates (TU and BU, respectively) occur at the same time for the VSCs whose

carriers are interleaved by 180°. However, due to the interleaving and the asymmetrical regular sampled method, the

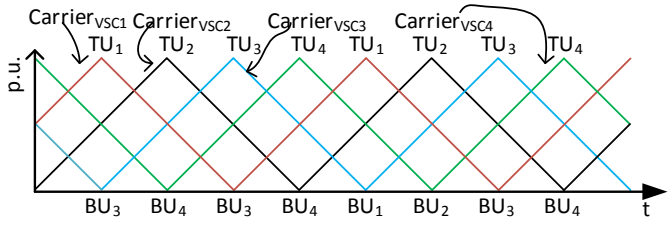


Fig. 2 Carriers, top and buttom updated of the four interlead VSCs

control algorithm is run at every 90°, so four times during a switching period.

## III. Circulating Current Control

PR controllers are used in the *abc* reference frame to control the fundamental component of the circulating current. The *abc* reference frame is used because all circulating currents have fundamental components, and therefore, there is no need for additional frame transformations when PR controllers are used.

In this article, an individual PR controller is used to control the circulating current between the corresponding phases. Because of this, a total of 9 controllers are used. The transfer function of the PR controller is:

$$G_{PR} = K_p + \frac{K_I s}{s^2 + \omega_o^2} \tag{2}$$

where $K_p$ is the proportional gain, $K_I$ is the integral gain, while $\omega_o$ is the resonance frequency.

The magnitude and phase of the fundamental component of the circulating current depends on the resistance mismatch between the phases. As a result, all of the fundamental components of these currents can be different. By using PR controllers, the positive and negative sequences of the circulating currents are controlled by having only one controller per phase. In every CG there is a need for three circulating current controllers and additional controllers are required to control the fundamental component of the circulating current between the CGs as well. However, the sampling and the time when these controllers have to be run may become cumbersome.

## IV. Sampling of the Circulating Current

If the circulating current controllers in the CGs are run and sampled four times per a switching cycle, it means that the sampled current will contain carrier frequency components and not just the fundamental one. The filtering of these sampled values can be a solution, however, the filtering would introduce significant delays in the signal and further complicate the control structure. Another, simpler solution is to use accurate sampling frequency. The circulating current for the CGs are sampled at the TU and BU of the corresponding VSCs, and the sampled value will only have the fundamental component. i.e. TU1 and BU1 for $CG_1$ and TU2 and BU2 for $CG_2$.

The major frequency component of the circulating currents between the CGs is at twice the carrier frequency. To avoid this frequency component in the sampled values, the circulating currents between the CGs have to be sampled at each TU and BU, meaning four times a carrier cycle.

The modulating signals fed to the VSCs are calculated based on the following information:

- Output of the total current controller;
- Output of the circulating current controller for the corresponding VSCs;
- Output of the circulating current controller between the CGs.

Between two VSCs, the output of the circulating current controller is divided by two and it is added to one of the VSCs, and it is subtracted from the other one in the same group. Similarly, the output of the circulating current controller between the CGs is divided by two and added to one of the CGs, and it is subtracted from the other CG as follows:

$$\begin{cases} M_{VSC1,x} = M_x + \dfrac{\mathrm{PR}_{CG1\_out,x}}{2} + \dfrac{\mathrm{PR}_{CG12\_out,x}}{2} \\ M_{VSC3,x} = M_x - \dfrac{\mathrm{PR}_{CG1\_out,x}}{2} + \dfrac{\mathrm{PR}_{CG12\_out,x}}{2} \\ M_{VSC2,x} = M_x + \dfrac{\mathrm{PR}_{CG2\_out,x}}{2} - \dfrac{\mathrm{PR}_{CG12\_out,x}}{2} \\ M_{VSC4,x} = M_x - \dfrac{\mathrm{PR}_{CG2\_out,x}}{2} - \dfrac{\mathrm{PR}_{CG12\_out,x}}{2} \end{cases} \tag{3}$$

where M is the output of the total current controller, $PR_{CG1\_out}$ and $PR_{CG2\_out}$ represent the output of the circulating current controller for the corresponding phase for $CG_1$ and $CG_2$, respectively, while $PR_{CG12\_out}$ is the output of the circulating current controller between $CG_1$ and $CG_2$.

## V. Simulation Results

To test the performance of the controllers a simulation model in PLECS has been implemented based on the schematic depicted by Fig. 1, and its' parameters are presented in **TABLE I**. Both the simulation and the experimental studies have been carried out on a resistive load with a modulation index of 1, resulting in nominal loading of the VSCs and the CIs. Resistance mismatches have been introduced in order to mimic the parameter variations previously presented. In this study three mismatches have been introduced with the following values:

- In CG2 between for phase V with a value of 2 Ω;
- Between the two CGs phase V with a value of 1.2Ω.

The circulating current between the two VSCs has two major frequency components: a high frequency and a fundamental frequency one. In this case the high frequency one is at the switching frequency, while the fundamental frequency one is due to the introduced additional resistance. These circulating currents produce magnetic flux in the CI, which also has the two above mentioned frequency components. Fig. 3

presents the three circulating currents and the produced flux in the CIs, when no circulating current controller is used. Both the circulating currents and the magnetic flux contain switching frequency and fundamental frequency components. The flux density in the CI should not exceed the saturation flux density of the CI. The fundamental component of the circulating current between $VSC_1$ and $VSC_3$ is ~0.32 A. The fundamental component in the flux produced by these currents is 0.19 T. On the other hand, the fundamental component of the circulating current between $CG_1$ and $CG_2$ is 1.89 A, while the corresponding flux in the CI is 1.25T.

**TABLE I SYSTEM PARAMETERS**

| Parameter | Value |
|---|---|
| Rated Power | 11kVA |
| Fundamental Frequency | 50 Hz |
| No. of VSCs | 4 |
| Interleaving angle | 90° |
| Switching Frequency | 1.95 kHz |
| Diff. mode inductor ($L_d$) | 2.3 mH |
| Inductance of the CI between 2 VSCs($L_{CI}$) | 75 mH |
| Inductance of the CI between 2 CGs($L_{CI,12}$) | 50 mH |
| Fundamental frequency | 50Hz |
| Fundamental current ($I_{TX}$) | 20 A (peak) |
| dc-link voltage | 650V |
| $R_{load}$ | 16.4Ω |
| Modulation method | SVM |
| Modulation index | 1 |

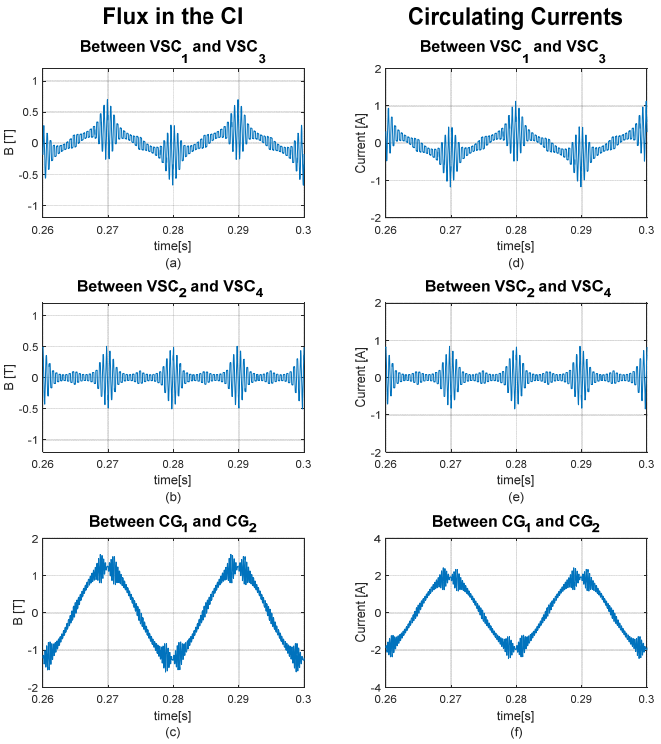


Fig. 3 Magnetic flux in the CI and circulating currents, when no circulating controller is used; a) Magnetic flux in the CI between $VSC_1$ and $VSC_3$; b) Magnetic flux in the CI between $VSC_2$ and $VSC_4$; c) Magnetic flux in the CI between $CG_1$ and $CG_2$; d) Circulating current between $VSC_1$ and $VSC_3$; e) Circulating current between $VSC_2$ and $VSC_4$; d) Circulating current between $CG_1$ and $CG_2$;

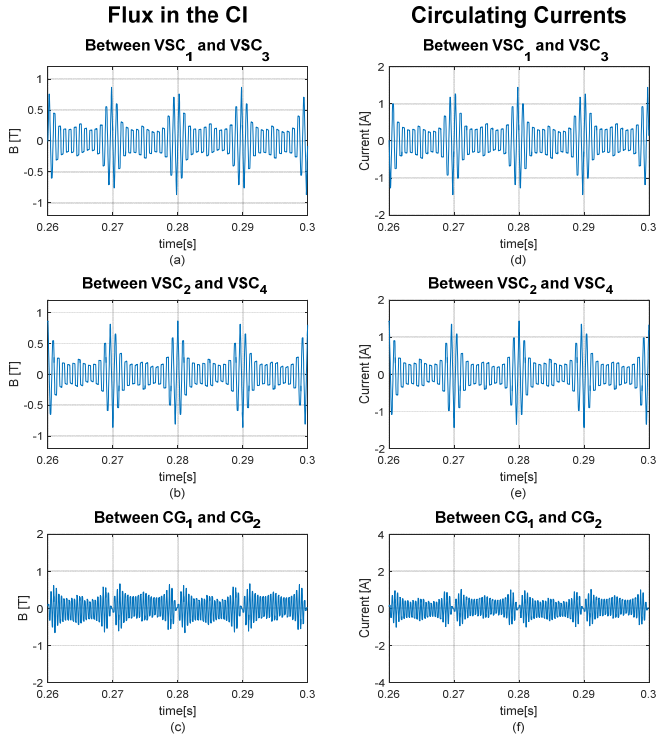


Fig. 4 Circulating currents and magnetic flux in the CI, when circulating controller is employed; a) Magnetic flux in the CI between $VSC_1$ and $VSC_3$; b) Magnetic flux in the CI between $VSC_2$ and $VSC_4$; c) Magnetic flux in the CI between $CG_1$ and $CG_2$; d) Circulating current between $VSC_1$ and $VSC_3$; e) Circulating current between $VSC_2$ and $VSC_4$; d) Circulating current between $CG_1$ and $CG_2$;

If the circulating current controllers are activated, the fundamental frequency component of the circulating current and inherently the flux in the CIs are reduced, as depicted by Fig. 4. The fundamental components of the circulating currents in $CG_1$ and in $CG_2$ have been reduced to ~0 A, inherently the fundamental component of the flux in the CIs is also reduced to ~0 A. Similarly, the fundamental component of the circulating current between the CG groups has also been reduced to ~0 A.

The simulation results prove that the proposed controller can effectively eliminate the low frequency circulating current, not only between the two VSCs, but also between the CGs, hence ensuring a stable operation of the VSCs.

## VI. EXPERIMENTAL RESULTS

The performance of the circulating current controllers was tested on an 11kVA setup, which consisted of four parallel interleaved VSCs. The VSCs were interconnected by CIs joined in a whiffletree configuration, as presented in Fig. 1. The parameters of the experimental setup are presented by TABLE I.

During the experimental study, resistances have been introduced into the path of the leg and group currents, which represent the parameter mismatches. It is to be noted that these values have been magnified in order to emphasize the

performance of the circulating current controllers. The resistances have been introduced between:

- In CG2 between for phase V with a value of 2 Ω
- Between the two CGs phase V with a value of 1.2Ω

The three circulating currents are presented by Fig. 5 for the case when no circulating current controller is employed. The magnitude of the fundamental frequency component of the circulating current is 0.23 A for $I_{B1,c}$, $I_{B2,c}$ is 1.03 A, and for $I_{B2,c}$ is 0.71A, respectively. The corresponding phase currents are shown on Fig. 6. A second set of measurements have been carried out for the case when the circulating current controllers has been enabled. The circulating currents, for this case, are shown on Fig. 7. It has to be noted that the fundamental frequency component of the circulating currents have been reduced significantly. In this case the fundamental component of the circulating currents has been reduced to 0.1 A for $I_{B2,c}$ and to 0.37 A for $I_{B2,c}$, respectively. As for the phase currents, which are depicted on Fig. 8, there is no change compared to the case when the circulatating current hasn't been employed.

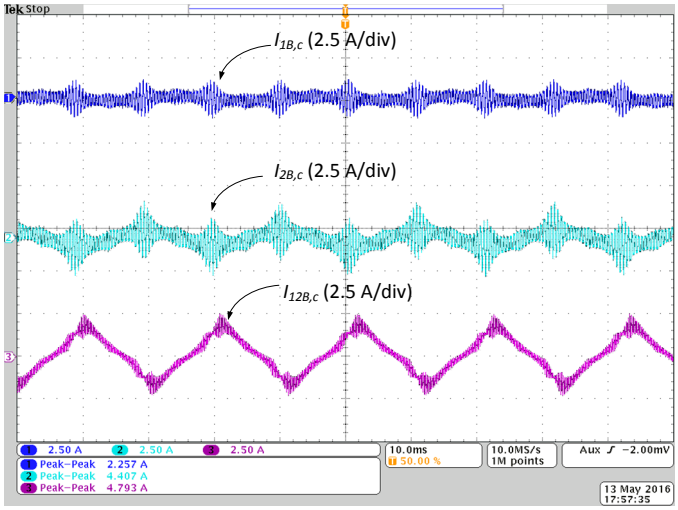


Fig. 5 Experimental results when no circulating current controller is employed for phase V: Circulating current between $VSC_1$ and $VSC_3$; b) Circulating current between $VSC_2$ and $VSC_4$ c) Circulating current between $CG_1$ and $CG_2$

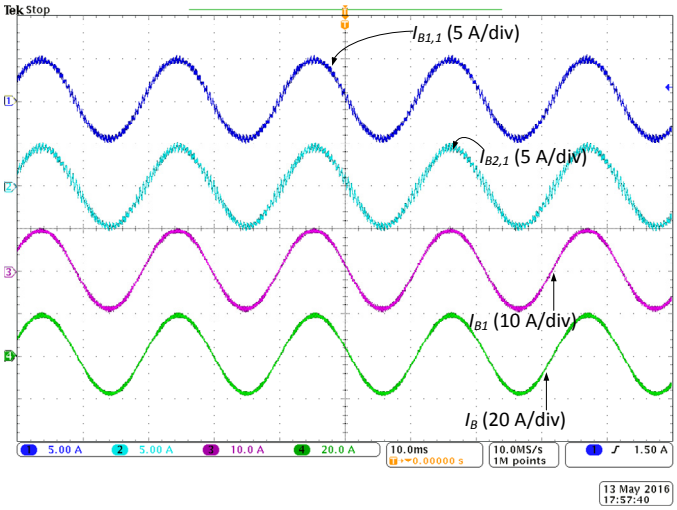


Fig. 6 Experimental results when no circulating current controller is employed for phase V: Phase current of $VSC_1$ ($I_{1B}$); b) Phase current of $VSC_2$ ($I_{2B}$) ; c) Sum of the phase currents for $VSC_1$ and $VSC_3$ ($I_B$); d) Total current ($I_{TB}$).

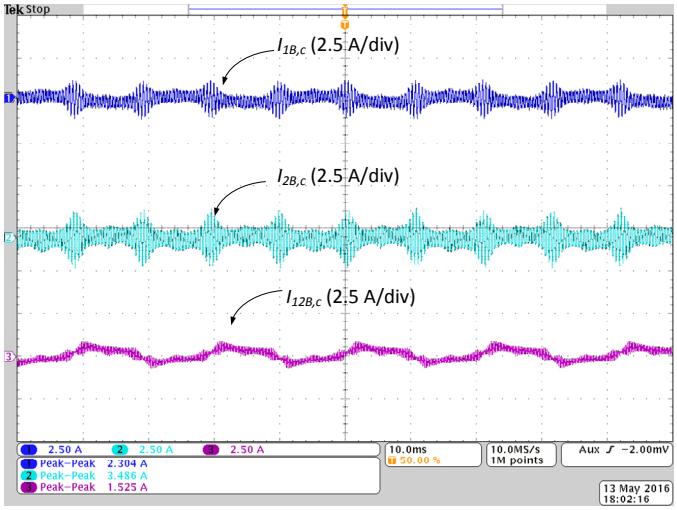


Fig. 7 Experimental results when circulating current controller is employed: Circulating current between $VSC_1$ and $VSC_3$; b) Circulating current between $VSC_2$ and $VSC_4$ c) Circulating current between $CG_1$ and $CG_2$

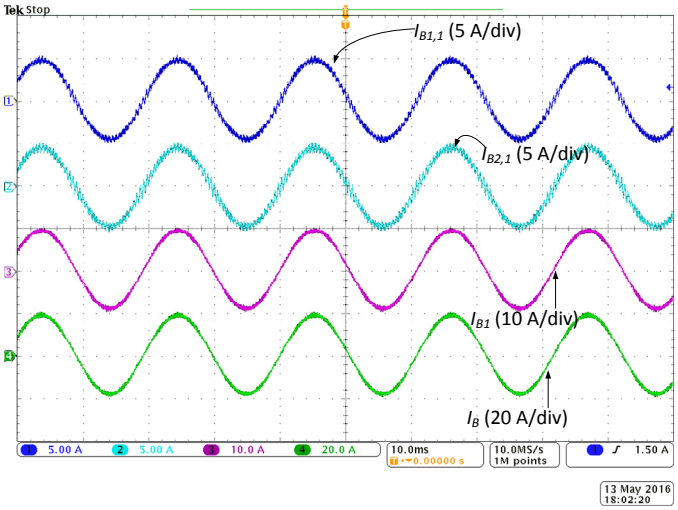


Fig. 8 Experimental results when circulating current controller is employed: Phase current of $VSC_1$ ($I_{1B}$); b) Phase current of $VSC_2$ ($I_{2B}$) ; c) Sum of the phase currents for $VSC_1$ and $VSC_3$ ($I_B$); d) Total current ($I_{TB}$).

## VII. CONCLUSIONS

This paper presented a method to control the fundamental frequency circulating currents in a parallel interleaved VSCs connected in a whiffletree configuration. The CIs used for the circulating current suppression and the presence of fundamental frequency flux component may result in the saturation of the CI. The proposed controller effectively eliminates the fundamental frequency component in the circulating current that flows between the VSCs and between the CGs. The experiment was performed by introducing mismatch in the parallel VSC system. In the case when no controller is used for the circulating current, the fundamental frequency component in the circulating current between the VSCs is 0.41 A, and between the CGs is 1.35 A. Using the proposed controller the fundamental component of the circulating current between the VSCs is reduced to 0.1 A, similarly the fundamental component of the circulating current between the CGs is also eliminated to 0.37 A. As a result, saturation free operation of the CI is achieved without oversizing it.

## REFERENCES


[1] (2015). *New record-breaking year for Danish wind power*. Available: http://energinet.dk/EN/El/Nyheder/Sider/Dansk-vindstroem-slaar-igen-rekord-42-procent.aspx

[2] B. B. d. Energieund and Wasserwirtschaft e.V., "Technical guidline: Generating plants connected to the medium-voltage network," ed, 2008.

[3] F. Blaabjerg, M. Liserre, and M. Ke, "Power Electronics Converters for Wind Turbine Systems," *Industry Applications, IEEE Transactions on,* vol. 48, pp. 708-719, 2012.

[4] S. AG. (2015). *Siemens D7 platform – 6.0-MW and 7.0-MW direct drive windturbines*. Available: http://www.energy.siemens.com/hq/pool/hq/power-generation/renewables/wind-power/platform brochures/D7-Platform-brochure_en.pdf

[5] V. W. Systems. (2011). *V164 8.0 MW*. Available: http://nozebra.ipapercms.dk/Vestas/Communication/Productbrochure/V16480MW/V16480MW/

[6] J. S. S. Prasad and G. Narayanan, "Minimization of Grid Current Distortion in Parallel-Connected Converters Through Carrier Interleaving," *Industrial Electronics, IEEE Transactions on,* vol. 61, pp. 76-91, 2014.

[7] G. Gohil, L. Bede, R. Teodorescu, T. Kerekes, and F. Blaabjerg, "Line Filter Design of Parallel Interleaved VSCs for High Power Wind Energy Conversion System," *Power Electronics, IEEE Transactions on,* vol. PP, pp. 1-1, 2015.

[8] G. Gohil, L. Bede, R. Teodorescu, T. Kerekes, and F. Blaabjerg, "Design of the trap filter for the high power converters with parallel interleaved VSCs," in *Industrial Electronics Society, IECON 2014 - 40th Annual Conference of the IEEE*, 2014, pp. 2030-2036.

[9] G. Gohil, L. Bede, R. Teodorescu, T. Kerekes, and F. Blaabjerg, "An Integrated Inductor For Parallel Interleaved Three-Phase Voltage Source Converters," *Power Electronics, IEEE Transactions on,* vol. PP, pp. 1-1, 2015.

[10] L. Asiminoaei, E. Aeloiza, P. N. Enjeti, and F. Blaabjerg, "Shunt Active-Power-Filter Topology Based on Parallel Interleaved Inverters," *Industrial Electronics, IEEE Transactions on,* vol. 55, pp. 1175-1189, 2008.

[11] J. W. Dixon and B. T. Ooi, "Series and parallel operation of hysteresis current-controlled PWM rectifiers," *Industry Applications, IEEE Transactions on,* vol. 25, pp. 644-651, 1989.

[12] G. J. Capella, J. Pou, S. Ceballos, J. Zaragoza, and V. G. Agelidis, "Current-Balancing Technique for Interleaved Voltage Source Inverters With Magnetically Coupled Legs Connected in Parallel," *Industrial Electronics, IEEE Transactions on,* vol. 62, pp. 1335-1344, 2015.

[13] D. Shin, K.-J. Lee, H.-J. Kim, J.-P. Lee, T.-J. Kim, and D.-W. Yoo, "Coupled inductors for parallel operation of interleaved three-phase voltage source grid-connected inverters," in *Applied Power Electronics Conference and Exposition (APEC), 2013 Twenty-Eighth Annual IEEE*, 2013, pp. 2235-2239.

[14] G. Gohil, L. Bede, R. Maheshwari, R. Teodorescu, T. Kerekes, and F. Blaabjerg, "Parallel interleaved VSCs: Influence of the PWM scheme on the design of the coupled inductor," in *Industrial Electronics Society, IECON 2014 - 40th Annual Conference of the IEEE*, 2014, pp. 1693-1699.

[15] G. Gohil, L. Bede, R. Teodorescu, T. Kerekes, and F. Blaabjerg, "Magnetic Integration for Parallel Interleaved VSCs Connected in a Whiffletree Configuration," *IEEE Transactions on Power Electronics,* vol. PP, pp. 1-1, 2016.

[16] G. Gohil, L. Bede, R. Teodorescu, T. Kerekes, and F. Blaabjerg, "An integrated inductor for parallel interleaved VSCs connected in a whiffletree configuration," in *Energy Conversion Congress and Exposition (ECCE), 2015 IEEE*, 2015, pp. 5952-5959.

[17] G. Gohil, L. Bede, R. Teodorescu, T. Kerekes, and F. Blaabjerg, "An Integrated Inductor for Parallel Interleaved VSCs and PWM Schemes for Flux Minimization," *Industrial Electronics, IEEE Transactions on,* vol. PP, pp. 1-1, 2015.

[18] G. Gohil, L. Bede, R. Teodorescu, T. Kerekes, and F. Blaabjerg, "Integrated inductor for interleaved operation of two parallel three-phase voltage source converters," in *Power Electronics and Applications (EPE'15 ECCE-Europe), 2015 17th European Conference on*, 2015, pp. 1-10.

[19] R. Maheshwari, G. Gohil, L. Bede, and S. Munk-Nielsen, "Effect of dead-time in interleaved PWM for two parallel-connected inverters," in *Power Electronics and Applications (EPE'15 ECCE-Europe), 2015 17th European Conference on*, 2015, pp. 1-7.

[20] L. Bede, G. Gohil, M. Ciobotaru, T. Kerekes, R. Teodorescu, and V. G. Agelidis, "Circulating current controller for parallel interleaved converters using PR controllers," in *Industrial Electronics Society, IECON 2015 - 41st Annual Conference of the IEEE*, 2015, pp. 003997-004002.

[21] R. Teodorescu, F. Blaabjerg, M. Liserre, and P. C. Loh, "Proportional-resonant controllers and filters for grid-connected voltage-source converters," *IEE Proceedings - Electric Power Applications,* vol. 153, pp. 750-762, 2006.

[22] B. P. McGrath and D. G. Holmes, "An analytical technique for the determination of spectral components of multilevel carrier-based PWM methods," *IEEE Transactions on Industrial Electronics,* vol. 49, pp. 847-857, 2002.